Experimental performance evaluation of a 5G spectrum sharing scenario based on field-measured channels

Oriol Font-Bach*, Nikolaos Bartzoudis*, David López*, Evgenii Vinogradov†,
Miquel Payaró*, Claude Oestges†,Tor Andre Myrvoll‡, Vidar Ringset‡
*Centre Tecnològic de Telecomunicacions de Catalunya (CTTC), Castelldefels, Barcelona, Spain
Email: {oriol.font, nikolaos.bartzoudis, david.lopez, miquel.payaro}@cttc.cat
†ICTEAM, Universitè Catholique de Louvain, Louvain-la-Neuve, Belgium
Email: {evgenii.vinogradov, claude.oestges}@uclouvain.be
‡SINTEF ICT, Trondheim, Norway
Email: {torandre.myrvoll, vidar.j.ringset}@sintef.no

***Abstract*—In this paper, an experimental performance evaluation is carried out within a communication scenario that features two of the key enablers of 5G: (i) the use of post-OFDM modulations and (ii) an efficient use of the spectrum via spectrum sharing. The experimental lab set-up has been assembled so as to operate in conditions as realistic as possible via the actual real-time implementation of the involved transceivers and also via the utilization of propagation channels which have been recorded in a field measurement campaign and which are loaded in a channel emulator that also operates in real-time. The experimental results show that co-existence in a shared spectrum scenario is possible and that the performance degradation is kept at a low level as long as one of the two users is making use of spectrally agile post-OFDM modulations such as filterbank multicarrier (FBMC).**

I. Introduction

While fourth generation (4G) wireless network deployments are still underway, a joint effort involving the entire industry and academic community is making steady progress towards the definition and specification of 5G systems, providing as well early proof-of-concepts and prototypes of key technology enablers. This paper focuses on two specific technology enablers of 5G wireless communication systems: **(i)** filter bank multi-carrier (FBMC) is a spectrally efficient waveform that is currently proposed to complement or enhance the current 4G long term evolution (LTE) technology [1]. Among other candidate waveforms, FBMC is being evaluated in the framework of different European Commission (EC) funded research projects focusing on 5G topics [2] [3]. **(ii)** Operators foresee that the efficient exploitation of the existing underutilized licensed spectrum is a means to sustain the anticipated increased traffic demands when 5G systems will start being deployed after 2020. Although the use of spectrum above 6 GHz for 5G radio access systems is gaining momentum, the Next Generation Mobile Networks (NGMN) Alliance clearly underlines that a flexibly utilized frequency spectrum below 6 GHz is absolutely essential for a cost-efficient delivery of mobile services in current and future 5G systems [1].

These two 5G technology enablers were combined in a FBMC downlink (DL) communication system that largely adopted the LTE specifications and frame structure, demonstrating promising results in terms of spectral efficiency and spectral contention (i.e., without compromising the performance of other adjacent or in-band transmissions [4]). In principle, the premium characteristics of FBMC in terms of spectral efficiency and interference protection to adjacent transmissions can be applied to a plethora of 5G end-use scenarios, where underutilized fragmented spectrum exists (licensed, unlicensed or a combination of the two).

In this paper we present an experimental analysis of the gains achieved when FBMC waveforms are used as secondary transmissions having as a goal to exploit the unused spectrum of other licensed narrowband primary transmissions. The assembled testbed allowed the performance evaluation of (a) a configurable DL FBMC system able to optimally utilize fragmented spectrum in a band where narrowband primary transmissions take place and (b) a point-to-point standalone DL FBMC system. Field-measured channels that were recorded employing a channel sounder in different indoor and outdoor configuration setups have been also used to increase the practical interest of the experimental analysis.

The remaining of the paper is organized as follows. The targeted 5G operating scenario is defined in Section II. In Section III, the channel measurement campaign is described. The broadband FBMC system is defined in Section IV. Likewise, the utilized hardware setup is described in Section V. The experimental analysis is presented in Section VI.

II. Target 5G scenario

The NGMN Alliance defines as a key 5G operating prerequisite the use of new flexible waveforms to effectively exploit underutilized licensed and unlicensed spectrum below 6 GHz [1]. Optimal spectral contention of the fragmented spectrum is required for these new waveforms in order to ensure a non-interfering coexistence with other signals (either in-band or at the edges of adjacent bands). Due to the high

978-1-4673-6782-0/15/$31.00 ©2015 IEEE

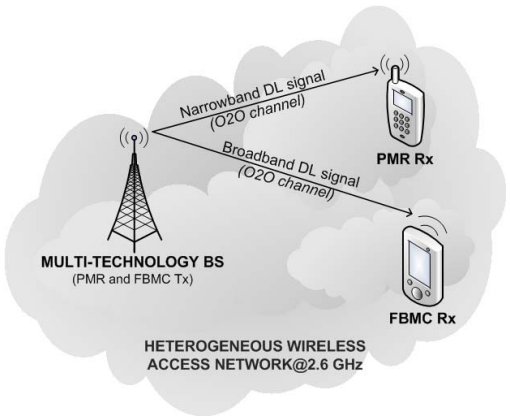

(a) Outdoor deployment. Setup and frequencies were selected for demonstration purposes only.

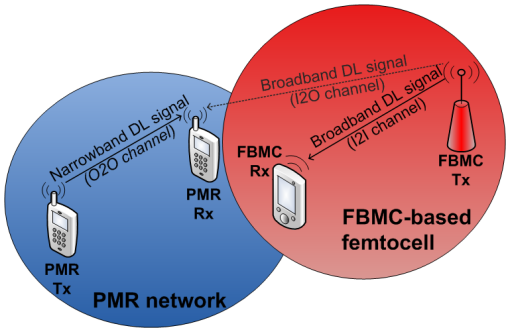

(b) Heterogeneous network deployment.

Fig. 1. Considered operating scenarios.

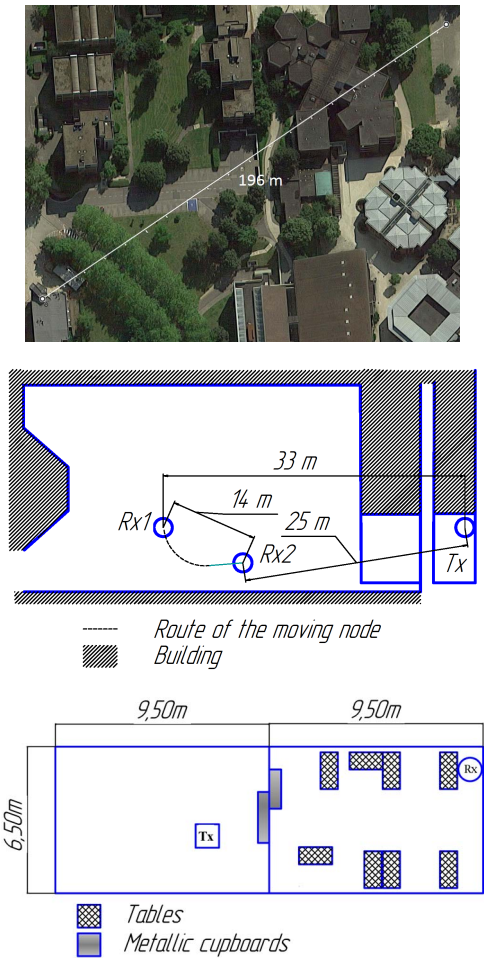

Fig. 2. Floor-plan of peer-to-peer measurements.

complexity involved with such experimental validation, a rather simple yet highly representative 5G operating scenario has been considered based on field measured channel data and a robust real-time DL communication system that was built and demonstrated as part of the EC-funded project EMPhAtiC [3]. The end use scenario features a primary narrowband professional mobile radio (PMR) transmission coexisting with a LTE-like opportunistic FBMC-based broadband transmission. Both systems are sharing the same frequency band and make use of a point-to-point DL communication link. Two different use cases were considered (Fig. 1): i) the coexisting narrowband and broadband systems are deployed outdoors and ii) the primary system is located outdoors, with its receiver (Rx) located at its cell's edge and near an indoor FBMC transmitter (Tx; e.g., femtocell network). In both use cases it is a hard requirement to dynamically adapt the FBMC signal so as not to interfere with the primary transmission. This is made feasible by deactivating subcarriers in the broadband transmission. The FBMC DL system is also capable of applying dynamic subacarrier allocation serving likewise cognitive radio use cases, but this feature is not covered in this paper. The diverse range of channel conditions considered by the two scenarios required the acquisition of realistic outdoors-to-outdoors (O2O), indoors-to-indoors (I2I) and indoors-to-outdoors (I2O) field-measurements, as it is detailed in the following section.

III. Field-measured channels

A. Equipment

The measurements were carried out using an Elektrobit PROPSound^{TM} channel sounder (CS). The Rx sensitivity is -88 dBm and a Rubidium clock reference in both Tx and Rx units ensured accurate timing and clock synchronization. The CS used long pseudo-noise (PN) sequences to estimate the impulse response of the radio channels between Tx and Rx nodes with the cycle rates listed in Table I, which also includes other parameters. As cycle rate, it is denoted the time-varying complex channel impulse response (CIR) matrix that was measured.

The only difference in the equipment used in each measurement scenario was the type of antennas:

1) I2I: custom-made dipole antennas with a gain of 1.75 dB and an omnidirectional radiation pattern were used. The nodes were connected with the channel sounder using long low-loss RF cables, which had equal length. The RF cables had excellent RF stability, even when they were slightly bent or moved during the measurements.
2) O2O and I2O: 2×4 dual-polarized ($\pm 45°$ slanted polarizations) planar array was used at the BS side. At

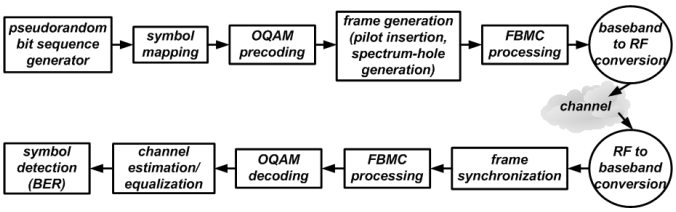

Fig. 3. Processing blocks of the FBMC system.

TABLE I
MEASUREMENT PARAMETERS

Parameter	O2O	I2I	I2O
Center frequency		3.8 GHz	
Transmit power		23 dBm	
Measurement bandwidth		200 MHz	
Recorded time samples N_s		2000	
Code length	5.11 μs	10.23 μs	2.55 μs
Number of channels	64	1	64
Cycle Rate	30.4 Hz	99.7 Hz	104.7 Hz

the MS side, we used an omnidirectional circular array made of 8 vertically-polarized dipoles (gain of 2 dB). So that, 8×8 MIMO channels were measured (i.e., 64 links).

To use the measured CIRs in the channel emulator, the routine described in [6], [7] was applied with the following parameters:

- Number of used paths: 49
- Methods to remove paths: Minimum Energy Error
- Data interpolation factor: 20

Taking into account the specifications of the equipment used in the real-time testbed (see Section V), the CIR data-files were appropriately adjusted to be used at the (4G LTE) 2.595 GHz RF band. This frequency-scaling was carried out by assuming that the baseband power-delay profiles are carrier-frequency-independent. While this assumption could be unrealistic with respect to the instantaneous CIRs, in this experimental validation it is not affecting the obtained results since the target performance metric is the average performance and not the instantaneous one (i.e. the temporal statistics of the channel remain similar).

B. Environment

The field-captures are based on three channel measurement campaigns carried out at the Université Catholique de Louvain (UCL), Louvain-la-Neuve, Belgium. The investigated outdoor environment was located in the campus area and consists of three-to-four storey office buildings, parking lots and relatively narrow streets. The area is characterized by small tree density and pedestrian traffic. The investigated indoor environment is a typical office building that consists of rooms along a corridor separated by brick walls as shown in Fig. 2.

I2I: The Rx node was moving in random directions over a small area within a square of 1 m^2 with a walking speed of $v \approx 1$ m/s), while the Tx was static. The floorplan of the office

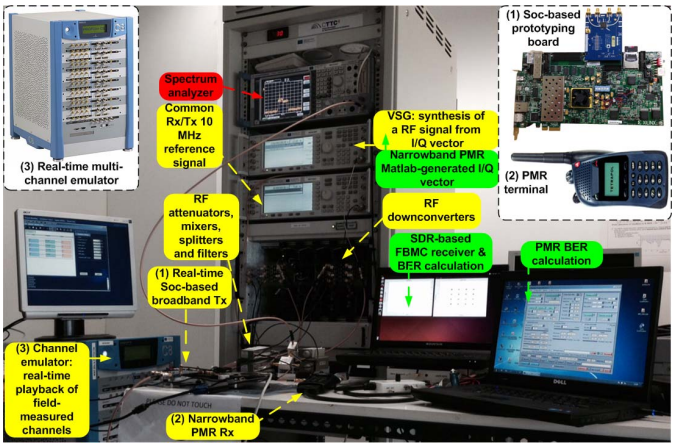

Fig. 4. Laboratory setup with detail of the SoC-based prototyping board, PMR terminal and channel emulator.

is showed Fig. 2 (bottom). The distance between the nodes is 12 m.

I2O: At the MS side, the antenna was mounted at the height of 2m on a fixed mast attached to a trolley moving with a pedestrian speed ($v \approx 1$ m/s). The trolley was moving along a parking with no moving cars during the channel measurement (Fig. 2 middle). The BS was at the ground floor of an office building. The distance between the nodes was varying during the measurement between 25 – 33 m.

O2O: The BS was fixed at the top of a four-storey building at the height 20 m above the local ground level. The moving trolley again was used as the MS. The measured area is under NLOS conditions due to dense building blockage. The distance between the nodes was varying during the measurement between 190 – 205 m.

IV. OVERVIEW OF THE DL FBMC SYSTEM

A. FBMC scheme

The FBMC system uses a fast-convolution (FC) multirate filter bank scheme described in [8], which yields an efficient and flexible FBMC implementation. The frame structure of the FBMC/offset quadrature amplitude modulation (OQAM) DL signal is based on the equivalent LTE configuration for 1.4 MHz BW. 72 active subcarriers (i.e., 15 kHz spacing) are included in each FBMC symbol for a total 10 ms long radio frame comprising 150 FBMC symbols. Channel coding was not implemented and all user-data symbols were mapped onto a 16-QAM constellation. The FBMC frame contains a preamble for synchronization purposes, which guarantees correct operation under fragmented spectrum situations [5]. At the Rx the channel estimation utilizes a pilot pattern resembling that of LTE. The precise values of the imaginary part of the latter were calculated using the surrounding data in order to compensate its coupling with the actual pilot symbol. A block diagram of the FBMC system is shown in Fig. 3.

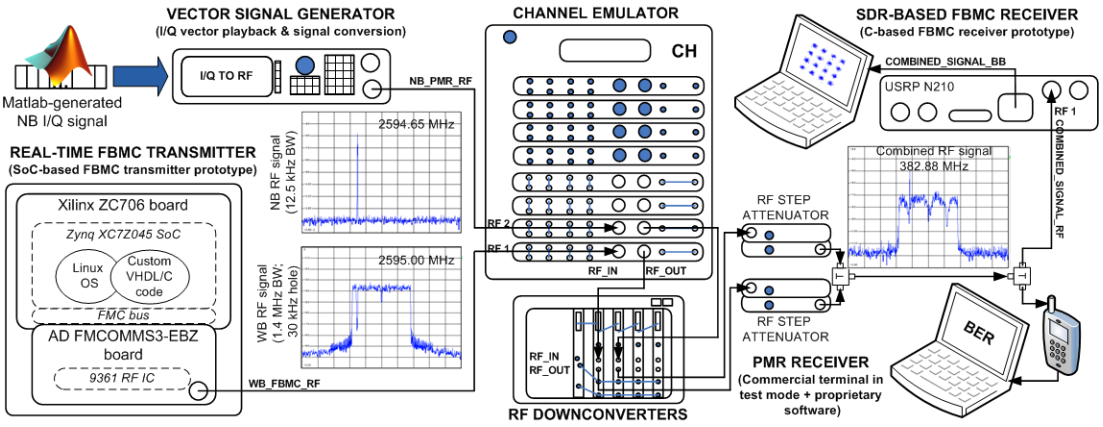

Fig. 5. Hardware setup implementing the FBMC/PMR coexistence scenarios.

B. Baseband implementation approach

The key baseband processing requirements of future 5G wireless communication systems are flexibility, high computational capacity and low power consumption. A key enabling technology that guarantees the previous is the hardware-assisted software defined radio (SDR), which augments the advantages of software-based PHY-layer implementations by accelerating the bit-intensive digital signal processing (DSP) functions in field programmable gate arrays (FPGA) devices. Hybrid baseband processing devices that combine hardware accelerators in programmable logic with a general purpose embedded multi-core processor in a single chip architecture, satisfy both flexible SDR functionality and massive parallelism. Apart from the functional and technology advantages, such FPGA-based system-on-chip (SoC) devices are optimized for performance, reducing at the same time both the component cost and the energy consumption, making them an ideal candidate for 5G baseband signal processing implementations.

Two different SDR-based approaches have been thus utilized to implement the DL FBMC Tx and Rx. The receiver system made use of a traditional SDR implementation targeting a general purpose computer (GPC). In more details, the software implementation was based on the IRIS SDR framework [9], which facilitates a dataflow structure where the different DSP stages can be represented as a graph. Whilst the upper-bound performance limit of GPCs forced the selection of baseline DSP algorithms (e.g., no channel coding was implemented and a linear interpolation was used in the channel estimation block), it has been shown that it was possible to implement a real-time FBMC receiver by combining efficient programming techniques and a modern multi-core GPC. At the transmitter side, a hardware-assisted SDR (i.e., hardware-software co-design) approach was selected targeting a FPGA-based SoC device. An optimized custom digital design, combining latency-aware storage, resource sharing and other advanced register transfer level (RTL) design features, enabled the efficient implementation of the FBMC transmitter. Furthermore, dynamic reconfiguration of the transmitted FBMC signal (i.e., dynamic subcarrier allocation) was also implemented. The embedded processor runs a distribution of the Ubuntu Linux operating system for ARM processors and a kernel-space software application is responsible for various control functions, especially focusing on the interactions of the SoC with the RF front-end.

V. The Real-Time Hardware Testbed Setup

A heterogeneous hardware setup was used to deploy the real-time demonstrator which was configured as (see Fig. 5):

- A vector signal generator (VSG) is used to emulate in real-time the primary narrowband PMR transmission. The VSG cyclically repeats a TETRAPOL I/Q frame-sequence (generated in Matlab) and synthesizes the RF signal centered at 2594.65 MHz. This signal enables the computation of the Bit Error Rate (BER) at the TETRAPOL terminal.
- The FBMC transmitter uses the Xilinx ZC706 board for the real-time baseband processing and the Analog Devices AD-FMCOMMS3-EBZ RF transceiver board for the RF up-conversion. The ZC706 board features the Xilinx XC7Z045 FPGA-based SoC device, whereas the RF front-end makes use of the AD9361 RF IC from Analog Devices, which provided the RF signal centered at 2.595 GHz.
- Both RF signals were fed to the Elektrobit Propsim C8 multi-channel emulator which plays back in real-time the field-measured channels required to deploy each operating scenario.
- The RF-downconversion utilized the Mercury Computer Systems Echotek Series RF 3000T Tuners which translated the two resulting RF signals at the output of the channel emulator from 2.595 GHz to the 380-400 MHz PMR band (i.e., centered at 382.88 MHz for the FBMC system and at 382.53 MHz for the PMR one).
- The downconverted RF signals were driven through a series of RF step attenuators which allowed to fully control the power ratio between the two coexisting transmissions.
- The power-adjusted RF signals were combined into a single RF signal. An in-house RF filter was additionally

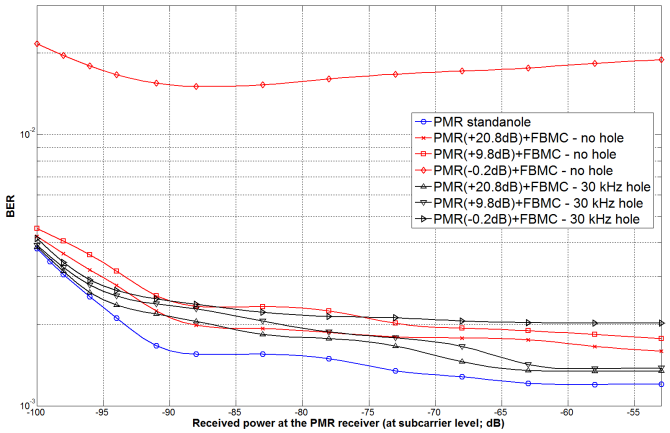

Fig. 6. Outdoor PMR performance, for different relative transmission powers in relation to an outdoor FBMC system.

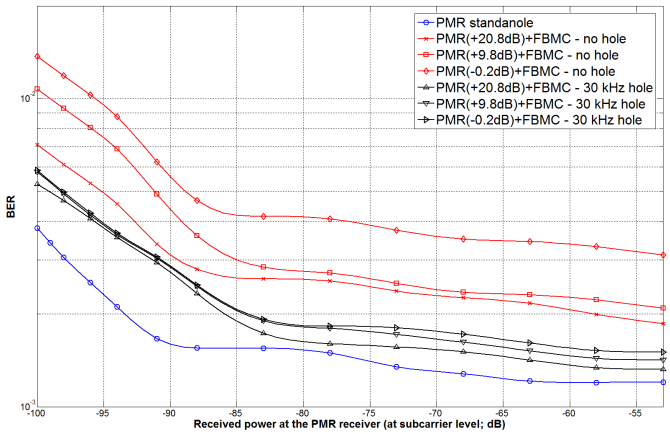

Fig. 7. Outdoor PMR performance, for different relative transmission powers in relation to an indoor FBMC system.

used to eliminate undesired out-of-band components. A RF splitter was added to provide two exact replicas of the combined RF signal. The replicas were then fed to the FBMC and PMR receivers.

- A M9620SG2 TETRAPOL terminal device configured in test mode acted as the PMR receiver for the primary transmission. The TETRAPOL terminal is interfaced through a custom cable with a computer, where a software application was used to calculate the averaged BER for a given number of frames.
- The FBMC receiver uses the Ettus Research USRP N210 device which after the RF signal down conversion, the signal acquisition and the digital down conversion, it provides the complex baseband samples to a GPC through a dedicated Gigabit Ethernet (GigE) interface. The SDR implementation of the FBMC receiver runs on a laptop, where the frame-based BER metrics are calculated.

A photo of the complete hardware setup comprising the real-time testbed is shown in Fig. 4.

VI. Measurement Campaign

An exhaustive measurement campaign was conducted to obtain a realistic performance analysis, applying the field-measured channels on the previously described hardware setup and considering different power ratios between the transmissions of the coexisting PMR and FBMC systems. In all deployed operating scenarios, the demonstrator equipment were carefully calibrated to attain different relative mean output power levels between the PMR and FBMC signal transmissions, allowing to meet the subcarrier power level ratios of the experimental evaluation presented in the following subsection. More specifically, the considered system configurations were ranging from an ideal situation where the PMR subcarrier power was 21 dB above that of the broadband one at the reception side, to an extreme case where the same subcarrier power level was observed for both primary and interfering signals. These power-relations were carefully selected based on the considered operating scenarios and the 3GPP pathloss model for suburban deployment of femtocells [10].

A. Experimental results

For each implemented testing scenario the BER was calculated by averaging the values obtained by 10.000 FBMC or PMR frames. It must be underlined that no channel coding is implemented in the FBMC system and consequently performance is measured in terms of uncoded (raw) BER. Each testing scenario was defined by combining specific configuration values regarding: a) the relative subcarrier power levels between the PMR and FBMC signals, b) the utilized field-measured channel and c) the FBMC subcarrier allocation. With respect to the latter, three different FBMC signal configurations were considered in order to illustrate the achieved gains in a spectrum coexistence scenario: i) the FBMC system is quiet (i.e., no interference is caused to the standalone PMR system), ii) the FBMC transmission allocates all 72 active subcarriers (i.e., maximum possible interference) and iii) 70 subcarriers are allocated in the FBMC signal, thus providing a 30 kHz spectrum-hole to accommodate the existing PMR 12.5 kHz signal.

Fig. 6 shows the performance at the PMR terminal when both coexisting wireless communication systems are deployed outdoors. Similarly, Fig. 7 considers an operating scenario where the FBMC system is deployed indoors. As it could be expected, minimal performance differences are observed in relation to the relative power levels of both coexisting transmission when a 30 kHz spectrum-hole is set in the FBMC signal. The performance of the PMR system is gradually degraded as the subcarrier power level of the PMR and FBMC signals is getting closer (without having counter-measures to tackle the DL interference). The figures provide a comparative insight of how the specific channel models that define a given operating scenario affect the performance of the wireless communication systems coexisting in it. In both coexistence scenarios though, the high spectral contention of the FBMC scheme is experimentally verified, guarantying likewise a

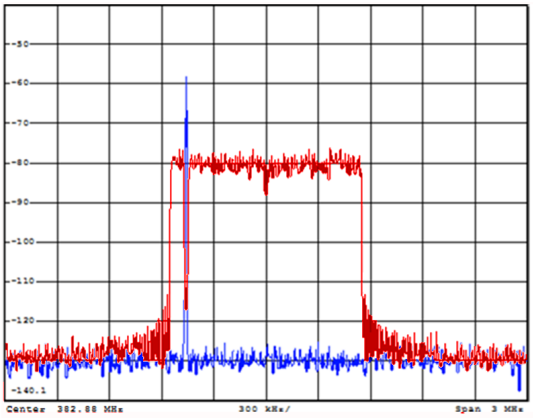

Fig. 8. Spectrum of the generated FBMC signal (prior to the upconversion stage), featuring a 30 kHz spectrum-hole, superposed to that of the PMR system.

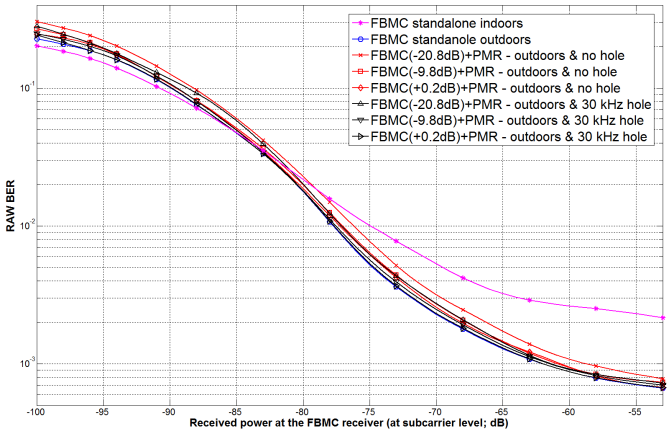

Fig. 9. Indoor and outdoor FBMC performance. For the latter, the impact of coexistence with an outdoor PMR system has also been characterized for different relative transmission powers.

minimal interference to other inband signals. This is also clearly observed in the spectrum plot of the FBMC signal shown in Fig. 8, where a 35 dB drop in the spectrum-hole was created to accommodate the primary PMR signal.

Fig. 9 shows the performance that was observed at the FBMC receiver when considering the reverse situation from the one described before (i.e., interference from the DL PMR signal) for the all-outdoor operating scenario. As expected, a marginal BER gain is still attained when a spectrum-hole is used (i.e., a 12.5 kHz may only impair a small number of channels in the FBMC signal). An interesting comparison point is provided by the introduction of the BER curve of a standalone indoor FBMC system. As it is expected, in the deployed scenarios, the measured channels have a greater impact on the performance of the multicarrier FBMC transmission, compared to that provoked by the narrowband interference.

VII. Conclusion

In the experimental evaluation reported in this paper, we have taken into account the features of a communications system that have a major impact on the BER performance such as the used waveforms (FC-FMBC, narrowband transmissions), the propagation channels (taken from a measurement campaign) and, also, the relevant interfering situation dictated by the corresponding considered scenarios (outdoor and heterogeneous network). For different configurations of the relation between the desired and interfering signal powers, it has been shown that co-existence in a shared spectrum scenario is possible and that the performance degradation is kept at a low level, provided that the waveform utilized by one of the two users is frequency agile. The experimental set-up assembled in this work will be used for further research work by endowing it with spectrum sensing and dynamic spectrum allocation capabilities so that more advanced features can also validated in such a realistic lab environment.

Acknowledgment

The authors would like to thank CASSIDIAN (Airbus Defence and Space) for kindly providing us with two PMR terminals and for their valuable support during the experimental validation and measurement campaign.

This work was partially supported by the Generalitat de Catalunya under grant 2014 SGR 1551; by the Spanish Government under project TEC2014-58341-C4-4-R; and by the European Commission under projects EMPhAtiC (GA 318362) and NEWCOM# (GA 318306).

References

[1] NGMN Alliance, “5G White Paper,” February 2015.

[2] G. Wunder, P. Jung, M. Kasparick, T. Wild, F. Schaich, C. Yejian, S. Brink, I. Gaspar, N. Michailow, A. Festag, L. Mendes, N. Cassiau, D. Ktenas, M. Dryjanski, S. Pietrzyk, B. Eged, P. Vago, F. Wiedmann, ”5GNOW: Non-Orthogonal, Asynchronous Waveforms for Future Mobile Applications”, IEEE Communications Magazine, Vol.52, Num.2, pp.97-105, February 2014.

[3] M. Renfors, D. Le Ruyet, D. Tsolkas, O. Font-Bach, N. Bartzoudis, P. Mege, L. Baltar, V. Ringset, X. Mestre, ”EMPhAtiC Intermediate Results and Standardization Strategy” *in Proceedings of the 23rd European Conference on Networks and Communications (EuCNC 2014)*, 23-26 June 2014, Bologna (Italy).

[4] EMPhAtiC D9.4, ”Evaluation of the implemented communication system”, February 2015.

[5] EMPhAtiC D9.1, ”Definition and specification of hardware demonstrator and software simulator”, March 2014.

[6] J. Kolu, T. Jämsä, A. Hulkkonen, ”Real Time Simulation of Measured Radio Channels” *in Proceedings of the 58th IEEE Vehicular Technology Conference (VTC 2003-Fall)*, 6-9 October 2003, Orlando, Florida (USA).

[7] Elektrobit Corporation, “Propsim channel models from measured data,” 2007.

[8] M. Renfors, J. Yli-Kaakinen, F.J. Harris, ”Analysis and Design of Efficient and Flexible Fast-Convolution Based Multirate Filter Banks”, IEEE Transactions on Signal Processing, Vol.62, Num.15, pp.3768-3783, August 2014.

[9] IRIS SDR framework webpage, https://github.com/softwareradiosystems.

[10] T. G. P. P. (3GPP), “Simulation assumptions and parameters for FDD HeNB RF requirements, 3GPP TSG RAN WG4 R4-092042,” 2009.